

Automatic Glaucoma Detection Method Applying a Statistical Approach to Fundus Images

Anindita Septiarini, Dr, Dyna M. Khairina, MKom, Awang H. Kridalaksana, MKom, Hamdani Hamdani, MCs

Department of Computer Science, Faculty of Computer Science and Information Technology, Mulawarman University, Samarinda, Indonesia

Objectives: Glaucoma is an incurable eye disease and the second leading cause of blindness in the world. Until 2020, the number of patients of this disease is estimated to increase. This paper proposes a glaucoma detection method using statistical features and the k-nearest neighbor algorithm as the classifier. **Methods:** We propose three statistical features, namely, the mean, smoothness and 3rd moment, which are extracted from images of the optic nerve head. These three features are obtained through feature extraction followed by feature selection using the correlation feature selection method. To classify those features, we apply the k-nearest neighbor algorithm as a classifier to perform glaucoma detection on fundus images. **Results:** To evaluate the performance of the proposed method, 84 fundus images were used as experimental data consisting of 41 glaucoma image and 43 normal images. The performance of our proposed method was measured in terms of accuracy, and the overall result achieved in this work was 95.24%, respectively. **Conclusions:** This research showed that the proposed method using three statistics features achieves good performance for glaucoma detection.

Keywords: Glaucoma, Retinal Degeneration, Optic Neuropathy, Fundus, Classification

I. Introduction

Glaucoma is an incurable disease that causes the sight degeneration, and it is the second leading cause of blindness in the

Submitted: September 7, 2017

Revised: 1st, October 17, 2017; 2nd, October 27, 2017

Accepted: November 4, 2017

Corresponding Author

Anindita Septiarini, Dr

Department of Computer Science, Faculty of Computer Science and Information Technology, Mulawarman University, Jalan Kuaro, Gn. Kelua, Samarinda Ulu, Kota Samarinda, Kalimantan Timur 75119, Indonesia. Tel: +62-81-551-45190, E-mail: anindita.septiarini@gmail.com

This is an Open Access article distributed under the terms of the Creative Commons Attribution Non-Commercial License (<http://creativecommons.org/licenses/by-nc/4.0/>) which permits unrestricted non-commercial use, distribution, and reproduction in any medium, provided the original work is properly cited.

© 2018 The Korean Society of Medical Informatics

world [1]. Until 2020, the number of glaucoma patients is expected to increase [2]. To observe the features of glaucoma, experts use several imaging modalities, including confocal scanning laser ophthalmoscopy (CSLO), Heidelberg retina tomography (HRT), optical coherence tomography (OCT), and fundus imaging [3]. Based on the imaging modality, several features of the retinal structure, such as the optic nerve head (ONH), cup, peripapillary atrophy, and retinal nerve fiber layer, need to be observed for glaucoma detection. In a fundus image, the ONH is a bright and rounded area, and there is a smaller, rounded area inside the ONH called a cup. Peripapillary atrophy appears as a crescent which coincides with the area outside the ONH. The retinal nerve fiber layer is also located outside the ONH, which has white striated textures. An overview of the structure of retina is shown in Figure 1A. To identify the features of glaucoma, two types of techniques can be applied. These techniques are based on structures that require segmentation or image-based features that require feature extraction [4,5].

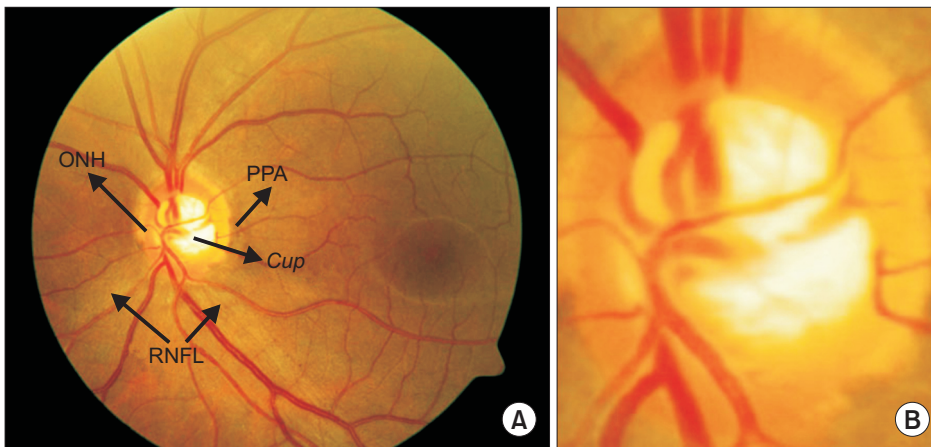


Figure 1. Examples of original image (A) and region of interest (ROI) image of optic nerve head (B). ONH: optic nerve head, PPA: parapapillary atrophy, RNFL: retinal nerve fiber layer.

Previous research related to glaucoma detection focused on the features of the ONH in fundus images has because the ONH is the main site affected by glaucoma. Before feature extraction can be performed on an ONH image, the process of ONH localization and segmentation is required. Localization is performed to form a sub-image that contains the region of interest in the ONH section. This sub-image is then called the region of interest (ROI) image, and it contains the whole ONH. The purpose of segmentation is to distinguish the ONH from the background. Several of the most popular methods involve processes of localization and segmentation, such as thresholding [6-8] and active contour [9,10]. Additional methods have been developed, such as superpixel [11] and fuzzy *c*-means [12]. These methods often misclassify the ONH area, so to overcome this morphological operations are applied [7-9,13]. An example original image and the result of the ONH detection process are shown in Figure 1A and 1B, respectively.

Several methods for texture feature extraction have been developed based on the ONH. Wavelet and higher-order spectra (HOS) methods are the most popular methods for feature extraction. Discrete wavelet transform (DWT) and HOS were applied with a support vector machine (SVM) classifier in [14]. Principal Component Analysis (PCA) was used to reduce the features obtained using DTW, and a probabilistic neural network (PNN) was used as the classifier [15]. PCA and SVM were performed in [16]. Subsequently, 18 features were produced by the wavelet method, and then the prominent method was applied for feature selection to provide the best features, followed by implementation of SVM and the *k*-nearest neighbor (*k*-NN) algorithm for classification [17]. Furthermore, the third-order HOS cumulant features and naïve-Bayesian (NB) classifiers were applied in [18]. The gray-level co-occurrence matrix (GLCM) method, the sequential forward floating selection (SFFS) technique,

and a backpropagation network (BPN) as a classifier were applied in [19]. In [20], the local binary pattern was used to obtain the representative texture features, which were classified using the *k*-NN algorithm. In addition to texture, shape features have been analyzed for glaucoma detection [21,22]. The implementation of shape feature analysis was proposed in [23] based on the cup and SVM contours.

The ONH is the main feature used to detect glaucoma. Therefore, research related to glaucoma detection based on the ONH is topic of great interest and is continually under development. Therefore, we propose an automatic glaucoma detection method that uses the texture feature in fundus images with a statistical approach, and the *k*-NN method is used for classification. The aim of this method is to determine whether the fundus image of a patient is normal or shows glaucoma. We used fundus images because fundus cameras are generally available in hospitals and eye care centers. Moreover, taking fundus images is inexpensive, and they can be used to check patients for other diseases, such as diabetic retinopathy, hypertension, and myopia.

The remainder of this paper is organized as follows. The datasets that used for the experiment and to test the proposed method are presented in Section II. The performance evaluation and the results of our experiment are discussed in Section III. Finally, Section IV presents a discussion of the results.

II. Methods

1. Datasets

This research used a total of 84 color fundus images (41 glaucoma and 43 normal), which were collected from two hospitals in Yogyakarta, and approval was obtained from the Ethics Committee (No. IRB KE/FK/1108/EC/2015). All the images were divided into two datasets because these images

were obtained by different tools. First, the Set-1 dataset was obtained from Dr. YAP Eye Hospital, and it contained 44 images taken by fundus camera (Carl Zeiss AG, Oberkochen, Germany) with a 30° field-of-view (FOV) and Nikon N150 digital camera (Nikon, Natori, Japan) with the resolution of 2240×1488 pixel. Second, the Set-2 dataset was obtained from Dr. Sardjito Hospital, and it contained 40 images taken using a 45° FOV Topcon TRC-NW8 fundus camera (Topcon Medical Systems Inc., Oakland, NJ, USA) and digitized at 4288×2848 pixels. Both datasets were provided in JPEG format. To evaluate our proposed method, an expert provided the label class (normal/glaucoma) for all the images. Forty-two sample images (19 glaucoma and 23 normal) were used in the stage of forming the features database, and 42 testing images (22 glaucoma and 20 normal) were used in the testing stage.

2. Proposed Method

This paper proposes a glaucoma detection method using a statistical approach on fundus images as the input data. The glaucoma detection result for each fundus image is either that it is normal or that it shows glaucoma. This method consists of two main stages, namely, forming the features database and testing. The main stages of our proposed method are presented in Figure 2.

The stage of forming the feature database requires two types of input information, namely, several sample fundus images and the label class (normal or glaucoma) of each image, while the testing stage requires only a fundus image as input data. There are two similar processes that are performed in both stages, namely, the process of forming an ROI image of the ONH and image enhancement. In

this work, an ROI image of the ONH is formed by using the method proposed in [8]. Furthermore, the focus of our method is image enhancement, feature extraction, and classification.

1) Forming an ROI image of the ONH

The goal of forming an ROI image of the ONH is to obtain a sub-image (see ④ of Figure 2) that has the same size as the ONH (height \times weight). This process comprises three main sub-processes, namely, localization, segmentation, and fitting the area of the ONH. First, we implement the process of localization. The input of localization is an original fundus image. Initially, thresholding based on the green channel of RGB with a high threshold is applied in to identify the approximate ONH center. We chose the green channel because the center of the ONH is more easily identified in this channel [13,23]. Subsequently, a border mask must be formed to overcome the noise that may occur at the border of the retina. Formation of the border mask comprises several steps: (1) thresholding based on the red channel of RGB by the Otsu method, (2) edge detection using the Sobel method, and (3) dilation. Then, we apply an AND operator against the result of thresholding based on the green channel and the border mask. Furthermore, the sub-image is formed based on the result of the AND operation (see ① of Figure 2).

Next, we carry out the sub-process of segmentation. Initially, median filtering is implemented in the red channel to suppress the influence of blood vessels, followed by thresholding using the Otsu method to segment the ONH from the background. We chose this channel because the ONH easily identified and segmented in the red channel [8,13]. To remove the non-ONH area that is classified as the ONH area,

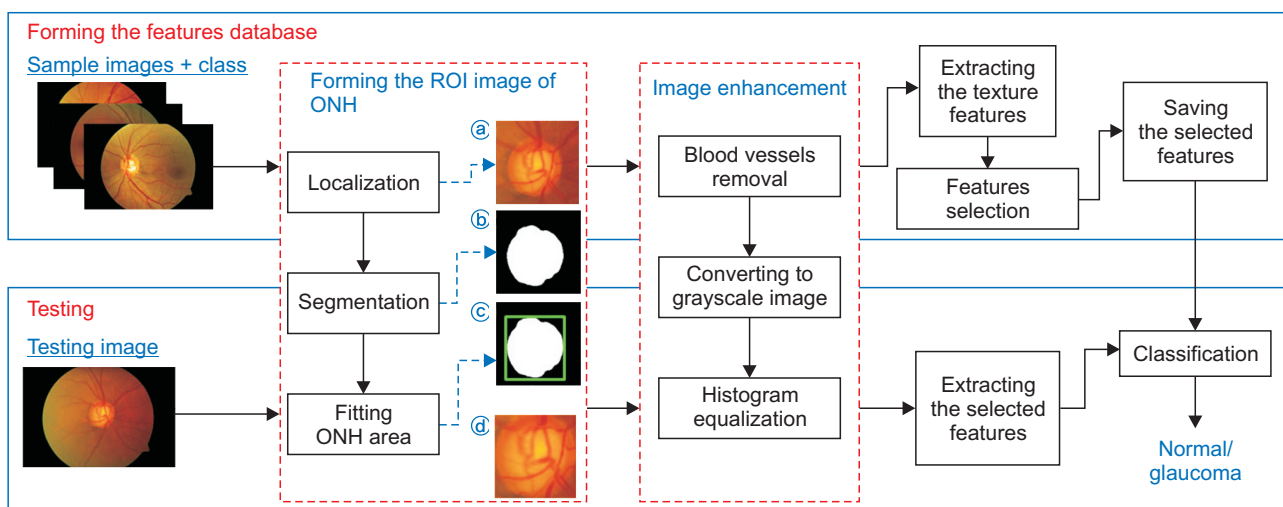


Figure 2. Main stages of our proposed method. ROI: region of interest, ONH: optic nerve head.

we apply as opening operation followed by dilation to obtain the correct size of the ONH. A segmentation result is shown in (a) of Figure 2. Finally, the sub-process of fitting the ONH area is carried out based on (b) of Figure 2 to obtain the size of the ROI image (see (c) of Figure 2), then the ROI image is set where the result is shown in (d) of Figure 2.

2) Image enhancement

The image enhancement process aims to improve the result of the subsequent process. In this work, we remove the blood vessels because they cover the area of the ONH by closing operation as in [8,23]. Subsequently, we convert the result of the previous step into a grayscale image followed by histogram equalization to increase the quality of the image.

3) Features extraction

(1) Stage: Forming the features dataset

In this stage, we compute six statistical features that are commonly used. They include the average intensity (mean), standard deviation, smoothness, 3rd moment, uniformity and entropy. Here, z_i is a random variable indicating the intensity value and $p(z_i)$ is the histogram with L intensity level in a region. All the features are defined as follows [24]:

- Mean

$$m = \sum_{i=0}^{L-1} z_i p(z_i) \quad (1)$$

- Standard deviation

$$\sigma = \sqrt{\mu_2(z)} = \sqrt{\sigma^2} \quad (2)$$

- Smoothness

$$R = 1 - \frac{1}{(1 + \sigma^2)} \quad (3)$$

- 3rd moment

$$\mu_3 = \sum_{i=0}^{L-1} (z_i - m)^3 p(z_i) \quad (4)$$

- Uniformity

$$U = \sum_{i=0}^{L-1} p^2(z_i) \quad (5)$$

- Entropy

$$e = \sum_{i=0}^{L-1} p(z_i) \log_2 p(z_i) \quad (6)$$

Not all of these extracted features play an important role in obtaining the optimal classification result in the next process. Therefore, dimensionality reduction of the features should be carried out through feature selection [25,26]. In this research, we implemented the correlation feature selection (CFS) method. This method was chosen because it has been applied in several studies, especially in the medical field [27-30].

CFS is a heuristic method that is used to compute the use of individual features to predicting the class with the level of inter-correlation among the features. The features that are highly correlated and irrelevant are discarded. To filter out irrelevant and redundant features that can lead to erroneous class predictions, we used the following equation [31]:

$$Fs = 1 - \frac{Nr_{ci}}{N + N(N-1)r_{jj}}, \quad (7)$$

where N is the number of features, r_{ci} is the mean feature correlation with the class, and r_{jj} is the average feature inter-correlation. Implementation of the CFS method in this work yielded only three selected features: mean, smoothness, and 3rd moment. Furthermore, saving the value of the selected features.

(2) Stage: Testing

In the testing stage, feature extraction is performed on a test image based on the selected features (mean, smoothness, and 3rd moment). Then, those selected features are used as the input data for the subsequent process of classification.

4) Classification

Classification is the final process in testing stage in which a decision is made determining whether the testing image falls into the class of normal or glaucoma. The inputs of classification are the values of mean, smoothness, and 3rd moment. We tested those features using several classifiers (k-NN, SVM, MLP, and NB) to obtain the optimal results. In our experiment, the k-NN classifier achieved better results than the other classifiers based on the dataset and features used.

The k-NN method is commonly used for classification because the process is simple. The k-NN algorithm requires several types of input data, such as the number of neighbor k , a distance matrix, and a dataset for training. If $k = 1$ then it is called the nearest neighbor classification, which determines the class of the test data based on the nearest neighbor of the training data. The distance matrix is calculated using the Euclidean distance (d), which is defined as [32]

$$d = \sqrt{\sum_{i=1}^c (x_i - y_i)^2}, \quad (8)$$

where i is the recurrence index, which is the number of features. The features matrix of the sample data is expressed by x_i , whereas that for the test data is y_i .

III. Results

The performance of our proposed glaucoma detection method is expressed in terms of sensitivity, specificity, and accuracy. Those values are defined as follows:

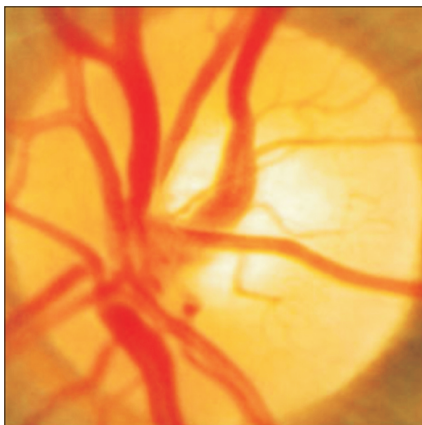
$$sensitivity = \frac{TP}{TP + FN}, \quad (9)$$

$$specificity = \frac{TN}{TN + FP}, \quad (10)$$

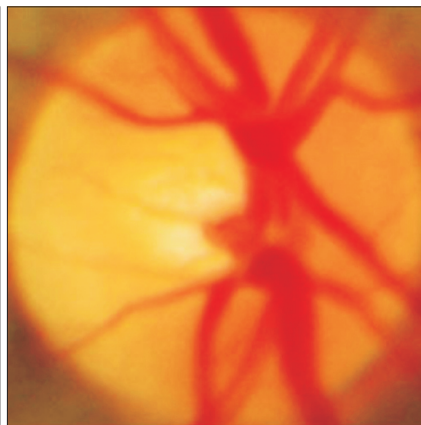
$$accuracy = \frac{TP + TN}{TP + TN + FP + FN}, \quad (11)$$

where

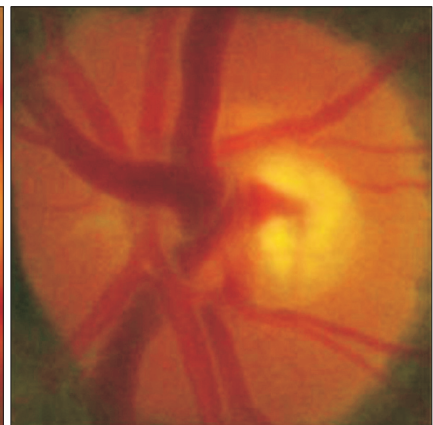
- True positive (TP) is the number images detected as glaucoma by an expert and the proposed method.
- True negative (TN) is the number of images detected as normal by an expert and the proposed method.
- False positive (FP) is the number of images detected as normal by an expert but detected as glaucoma by the proposed method.
- False negative (FN) is the number of images detected as



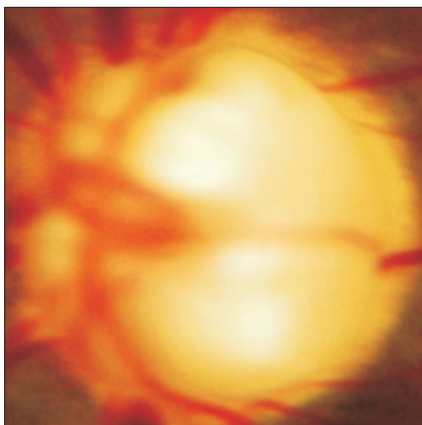
Class: normal
[Features value](#)
 Mean: 161.53
 Smoothness: 0.0023
 3rd moment: 0.1841



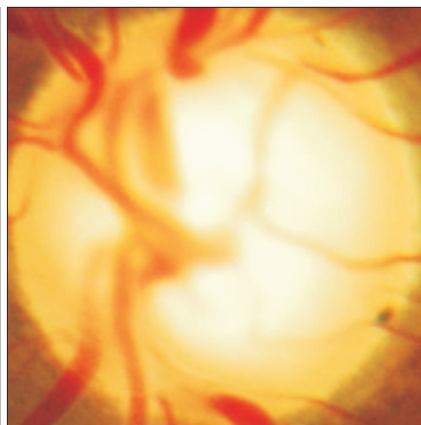
Class: normal
[Features value](#)
 Mean: 134.14
 Smoothness: 0.0021
 3rd moment: 0.2917



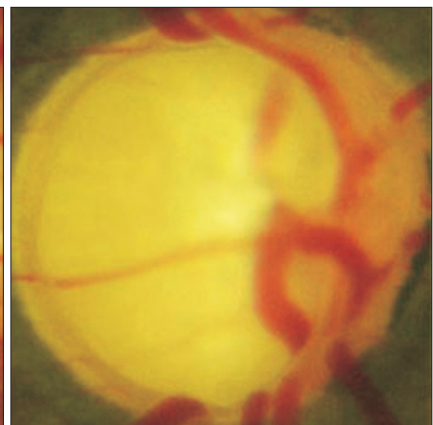
Class: normal
[Features value](#)
 Mean: 65.38
 Smoothness: 0.0073
 3rd moment: 0.1824



Class: glaucoma
[Features value](#)
 Mean: 152.25
 Smoothness: 0.0472
 3rd moment: -0.0768



Class: glaucoma
[Features value](#)
 Mean: 176.26
 Smoothness: 0.0417
 3rd moment: -1.1009



Class: glaucoma
[Features value](#)
 Mean: 109.91
 Smoothness: 0.0204
 3rd moment: -0.1476

Figure 3. Features extraction results of several images.

glaucoma by an expert but detected as normal by the proposed method.

The values of sensitivity, specificity, and accuracy lie between 0 and 1. Therefore, if the result of the proposed method is accurate, it should be close to 1.

The performance of our proposed method was evaluated by comparing the results of glaucoma detection provided by an expert based on observation of the ONH in fundus images and the classification results of our method using three features (mean, smoothness, and 3rd moment). The extraction results based on the ONH in several fundus images of the normal and glaucoma classes are presented in Figure 3.

Figure 3 shows the glaucoma detection results of the normal and glaucoma classes. There were differences between the obtained feature values of the normal and glaucoma classes. The mean value of the glaucoma class was higher than that of the normal class because of the enlargement of the cup area in the glaucoma eye, which caused the intensity value to increase. The enlargement of the cup area also caused the presence of blood vessels in the ONH to decrease, so that it affected the values of smoothness and 3rd moment. In the glaucoma class, the smoothness value was higher than that of the normal class. However, the 3rd moment value of the glaucoma class was lower than that of the normal class.

Each class has a different range of feature values. Erroneous

Table 1. Value ranges of features in the glaucoma and normal classes

Class	Mean	Smoothness	3rd moment
Glaucoma	101.35–200.97	0.0092–0.0472	–1.1009–0.3767
Normal	053.42–161.53	0.0021–0.0228	–0.0107–1.1448

classification results may occur if one or all of the features values of one class fall in the range of other classes. Based on the experimental results, the value ranges of features (mean, smoothness, and 3rd moment) in the normal and glaucoma classes are summarized in Table 1.

Based on Table 1, the following is an example illustrating how misclassification may occur. The values of mean, smoothness, and 3rd moment are 100.77, 0.0082, and –0.0247, respectively. The mean and smoothness values fall within the normal class range, but the 3rd moment value falls in the glaucoma class range.

The overall experimental results achieved by the proposed method are summarized in Table 2. Table 2 shows a comparison of classification results based on the proposed features using four different classifiers, namely, NB, MLP, SVM, and k-NN. The comparison was applied to obtain the optimal classification results. The classification results are expressed in terms of accuracy.

As seen in Table 2, that the proposed method successfully

Table 2. Comparison of classification results based on the proposed features using four classifiers

Classifier	Sensitivity (%)	Specificity (%)	AUC	Accuracy (%)
Naïve Bayes	92.90	97.67	0.99	92.86
MLP	94.00	93.02	0.98	94.05
SVM	92.90	100	0.93	92.86
k-NN	95.12	95.35	0.93	95.24

AUC: area under the receiver operating characteristic curve, MLP: multilayer perception, SVM: support vector machine, k-NN: k-nearest neighbor.

Table 3. Performance comparison of proposed method with other methods

Ref.	Year	Feature extraction method	Classifier	Datasets	Accuracy (%)
Noronha et al. [18]	2014	Higher order spectra	Naïve Bayes	272 images (100 normal, 172 glaucoma)	97.06
Ali et al. [20]	2014	Local binary pattern	k-NN	41 images (28 normal and 13 glaucoma)	95.10
Karthikeyan and Rengarajan [19]	2014	Gray level co-occurrence matrix	BPN	N/A	95.00
Singh et al. [17]	2016	Wavelet features	SVM and k-NN	63 images	94.70
Septiarini et al. [23]	2016	Contour feature based on the cup area	SVM	44 images (23 normal and 21 glaucoma)	94.44
Proposed method	2017	Statistical features (mean, smoothness and 3rd moment)	k-NN	84 images (43 normal and 41 glaucoma)	95.24

k-NN: k-nearest neighbor, BPN: back propagation network, SVM: support vector machine, N/A: not applicable.

detected the data of the normal class, achieving a specificity value of 95.35% based on the dataset used. Although there were differences in the detection results for the glaucoma class for all classifiers, k-NN achieved the best results, as indicated by the sensitivity value of 95.12%. Overall, the results presented in Table 2 demonstrate that the most appropriate classifier used in our proposed method was k-NN, which achieved an accuracy of 95.24% with the total experimental dataset comprising 84 images (43 normal and 41 glaucoma).

IV. Discussion

An automatic glaucoma detection method was developed using a statistical approach with the application of the k-NN classifier. The robustness of the proposed method was tested on several fundus images that were taken using two different cameras. The proposed method only uses three kinds of statistical features, namely, mean, smoothness, and 3rd moment, which were obtained through feature selection by the CFS method. Each feature has a unique range, as shown in Table 1; therefore, they are applied in the proposed method.

In this paper, we compared the results obtained by our proposed method with those of other methods to evaluate our method's performance, as shown in Table 3. Our method achieved an accuracy of 95.24%. In this research we used a smaller set of features than those used in other studies; however, the proposed method successfully detected all normal classes correctly and achieved greater accuracy than previous methods [17,19,20,23]. These results demonstrate that the proposed three statistical features can be applied to detect glaucoma. Nevertheless, it is lower than [18] because the detection results is related to the presence of blood vessels in the ONH area, and the feature values are influenced by the area size of the disc and cup. The proposed method has not been able to overcome the slight color differences color between the area of the disc and cup in that were present in several fundus images, and this caused some detection errors. To improve the performance of our method, it is necessary to combine the features extracted from fundus images with several clinical features of glaucoma.

In conclusion, this paper proposed a glaucoma detection method based on the analysis of fundus images using only three statistical features (mean, smoothness, and 3rd moment) and the k-NN classifier. In an experiment the proposed method successfully detected all normal class images correctly and achieved an accuracy of 95.24% This result proves that the three proposed statistical features are suitable for glaucoma detection. Based on the high accuracy

achieved, the proposed method with a statistical approach can make a valuable contribution to medical science by supporting medical image analysis for glaucoma detection. In future work, various features can be used or the features of texture, shape, and color can be combined to overcome the erroneous classifications and improve accuracy.

Conflict of Interest

No potential conflict of interest relevant to this article was reported.

Acknowledgments

The authors would like to thank Direktorat Riset dan Pengabdian Masyarakat (DRPM) RISTEKDIKTI Indonesia for the funding of research in the scheme of Penelitian Produk Terapan (PPT) in 2017 (No. 393/UN17.41/KL/2017).

References

1. Quigley HA. Number of people with glaucoma worldwide. *Br J Ophthalmol* 1996;80(5):389-93.
2. Quigley HA, Broman AT. The number of people with glaucoma worldwide in 2010 and 2020. *Br J Ophthalmol* 2006;90(3):262-7.
3. Gamero GE, Robert DF. The optic nerve in glaucoma. In: Choplin NT, Lundy D, editors. *Atlas of glaucoma*. 2nd ed. Boca Raton (FL): CRC Press; 2007.
4. Septiarini A, Harjoko A. Automatic glaucoma detection based on the type of features used : a review. *J Theor Appl Inf Technol* 2015;72(3):366-75.
5. Salam AA, Khalil T, Akram MU, Jameel A, Basit I. Automated detection of glaucoma using structural and non structural features. *Springerplus* 2016;5(1):1519.
6. Issac A, Partha Sarathi M, Dutta MK. An adaptive threshold based image processing technique for improved glaucoma detection and classification. *Comput Methods Programs Biomed* 2015;122(2):229-44.
7. Marin D, Gegundez-Arias ME, Suero A, Bravo JM. Obtaining optic disc center and pixel region by automatic thresholding methods on morphologically processed fundus images. *Comput Methods Programs Biomed* 2015;118(2):173-85.
8. Septiarini A, Harjoko A, Pulungan R, Ekantini R. Optic disc and cup segmentation by automatic thresholding with morphological operation for glaucoma evaluation. *Signal Image Video Process* 2017;11(5):945-52.

9. Muramatsu C, Nakagawa T, Sawada A, Hatanaka Y, Hara T, Yamamoto T, et al. Automated segmentation of optic disc region on retinal fundus photographs: comparison of contour modeling and pixel classification methods. *Comput Methods Programs Biomed* 2011; 101(1):23-32.
10. Mary MC, Rajsingh EB, Jacob JK, Anandhi D, Amato U, Selvan SE. An empirical study on optic disc segmentation using an active contour model. *Biomed Signal Process Control* 2015;18:19-29.
11. Cheng J, Liu J, Xu Y, Yin F, Wong DW, Tan NM, et al. Superpixel classification based optic disc and optic cup segmentation for glaucoma screening. *IEEE Trans Med Imaging* 2013;32(6):1019-32.
12. Khalid NE, Noor NM, Ariff N. Fuzzy c-means (FCM) for optic cup and disc segmentation with morphological operation. *Procedia Comput Sci* 2014;42:255-62.
13. Welfer D, Scharcanski J, Marinho DR. A morphologic two-stage approach for automated optic disk detection in color eye fundus images. *Pattern Recognit Lett* 2013; 34(5):476-85.
14. Mookiah MR, Acharya UR, Lim CM, Petznick A, Suri JS. Data mining technique for automated diagnosis of glaucoma using higher order spectra and wavelet energy features. *Knowl Based Syst* 2012;33:73-82.
15. Annu N, Justin J. Classification of glaucoma images using wavelet based energy features and PCA. *Int J Sci Eng Res* 2013;4(5):1369-74.
16. Dey A, Bandyopadhyay SK. Automated glaucoma detection using support vector machine classification method. *Br J Med Med Res* 2016;11(12):1-12.
17. Singh A, Dutta MK, ParthaSarathi M, Uher V, Burget R. Image processing based automatic diagnosis of glaucoma using wavelet features of segmented optic disc from fundus image. *Comput Methods Programs Biomed* 2016;124:108-20.
18. Noronha KP, Acharya UR, Nayak KP, Martis RJ, Bhandary SV. Automated classification of glaucoma stages using higher order cumulant features. *Biomed Signal Process Control* 2014;10(1):174-83.
19. Karthikeyan S, Rengarajan N. Performance analysis of gray level cooccurrence matrix texture features for glaucoma diagnosis. *Am J Appl Sci* 2014;11(2):248-57.
20. Ali MA, Hurtut T, Faucon T, Cheriet F. Glaucoma detection based on local binary patterns in fundus photographs. *Proceedings of SPIE Medical Imaging 2014: Image Processing*; 2014 Feb 16-18; San Diego, CA.
21. Aruchamy S, Bhattacharjee P, Sanyal G. Automated glaucoma screening in retinal fundus images. *Int J Multimed Ubiquitous Eng* 2015;10(9):129-36.
22. Murthi A, Madheswaran M. Medical decision support system to identify glaucoma using cup to disc ratio. *J Theor Appl Inf Technol* 2014;68(2):406-13.
23. Septiarini A, Hamdani, Khairina DM. The contour extraction of cup in fundus images for glaucoma detection. *Int J Electr Comput Eng* 2016;6(6):2797-804.
24. Sheshadri HS, Kandaswamy A. Breast tissue classification using statistical feature extraction of mammograms. *Med Imaging Inf Sci* 2006;23(3):105-7.
25. Kim TY, Son J, Kim KG. The recent progress in quantitative medical image analysis for computer aided diagnosis systems. *Healthc Inform Res* 2011;17(3):143-9.
26. Wiharto W, Kusananto H, Herianto H. Interpretation of clinical data based on C4.5 algorithm for the diagnosis of coronary heart disease. *Healthc Inform Res* 2016; 22(3):186-95.
27. Yousefi S, Goldbaum MH, Balasubramanian M, Jung TP, Weinreb RN, Medeiros FA, et al. Glaucoma progression detection using structural retinal nerve fiber layer measurements and functional visual field points. *IEEE Trans Biomed Eng* 2014;61(4):1143-54.
28. Ashraf M, Chetty G, Tran D, Sharma D. Hybrid approach for diagnosing thyroid, hepatitis, and breast cancer based on correlation based feature selection and Naïve Bayes. In: Huang T, Zeng Z, Li C, Leung CS, editors. *Neural Information Processing*. Heidelberg: Springer; 2012. p. 272-80.
29. Vanaja S, Kumar KR. Analysis of feature selection algorithms on classification : a survey. *Int J Comput Appl* 2014;96(17):28-35.
30. Saeyns Y, Inza I, Larranaga P. A review of feature selection techniques in bioinformatics. *Bioinformatics* 2007; 23(19):2507-17.
31. Hall MA, Smith LA. Feature selection for machine learning: comparing a correlation-based filter approach to the wrapper. *Proceedings of the 12th International FLAIRS Conference*; 1999 May 1-5; Orlando, FL. p. 235-9.
32. Kotsiantis SB. Supervised machine learning: a review of classification techniques. *Informatica* 2007;31:249-68.